Supramolecular Chirogenesis in Zinc Porphyrins: Investigation of Zinc−Freebase Bis-Porphyrin, New Mechanistic Insights, Extension of Sensing Abilities, and Solvent Effect

ARTICLE *in* THE JOURNAL OF PHYSICAL CHEMISTRY A · SEPTEMBER 2003

Impact Factor: 2.69 · DOI: 10.1021/jp034300p

4 AUTHORS, INCLUDING:

Victor Borovkov
Tallinn University of Technology
108 PUBLICATIONS **1,975** CITATIONS
SEE PROFILE

Yoshihisa Inoue
Osaka University
578 PUBLICATIONS **14,638** CITATIONS
SEE PROFILE

Supramolecular Chirogenesis in Zinc Porphyrins: Investigation of Zinc-Freebase Bis-Porphyrin, New Mechanistic Insights, Extension of Sensing Abilities, and Solvent Effect

Victor V. Borovkov,*,† Guy A. Hembury,† Naoyuki Yamamoto,‡ and Yoshihisa Inoue*,†

Entropy Control Project, ICORP, JST, 4-6-3 Kamishinden, Toyonaka, Osaka 560-0085, Japan, and Wako Pure Chemical Industries, Ltd., Hyogo, Japan

Received: February 5, 2003; In Final Form: June 10, 2003

The mechanism of supramolecular chirality induction in achiral ethane-bridged syn bis-porphyrins on interaction with chiral amines (L*) was investigated by comparison of bis(zinc porphyrin), **ZnZn** (possessing two binding sites), with zinc-freebase bis-porphyrin, **Zn2H** (possessing one binding site) in CH_2Cl_2 and CCl_4 solvents. UV−vis and CD analyses showed that the major contribution to the supramolecular chirality induction mechanism is the total number of supramolecular chiral steric interactions occurring in solution between the host's 3- and 7-ethyl groups and the guest bound only to the inside face of the host. This can be seen in that the full width at half-maximum (fwhm) values of the Soret band of **ZnZn**•L*$_2$ are significantly smaller than the **Zn2H**•L* species due to the presence of a higher percentage of species with chiral steric interactions which reduce the flexibility of the resulting complex. In the CD spectra the Cotton effects of **Zn2H**•L* are dramatically reduced by an average of 63% in comparison to **ZnZn**•L*$_2$, which is closer to the 75% expected on consideration of the number of supramolecular steric interactions than the 33% expected from the number of chirally active species. The same chirality-inducing steric mechanism can also be observed in the lower degree of supramolecular chirality induction observed for the **Zn2H**•L* system in CCl_4 than in CH_2Cl_2, with an average reduction of 45% in the CD intensity. The lower ability of CCl_4 to electrostatically interact with the ligand and porphyrin reduces the bulkiness of the corresponding substituents thus reducing the degree of chiral steric repulsion. This system possesses a high degree of chiroptical activity allowing the use of **Zn2H** for the determination of the absolute configuration of chiral ligands, by virtue of its one-point coordination property. Thus, it is possible to determine the absolute configuration of bis-amines, something not previously possible with **ZnZn**.

Introduction

Recently the study of chiral molecules and architectures has been a subject of significant multidisciplinary interest. In particular, the search for comprehensive facile and efficient generation and subsequent control of molecular and supramolecular chirality have resulted in this topic pervading numerous areas of frontier chemical, material, and biochemical sciences. Indeed, interest in these areas has led to the development of rationally designed functional molecules with specific properties able to perform highly efficient specialized tasks in areas such as catalysis,[1] nonlinear optics,[2] materials science,[3] and molecular device design.[4]

In all such systems the transfer of chirality plays the pivotal role, and as such the rationalization of the associated mechanism is of vital importance. Indeed there has been progress made in the more fundamental understanding of this process in a number of functional molecular systems.[5] However, the general level of understanding of the mechanisms by which structural molecular information is transferred between molecules (or within molecules), to-date, has been almost exclusively empirical in nature. This lack of detailed mechanistic understanding will, and indeed does, limit the development of this exciting and promising field. Thus, the rationalization of the mechanisms of chirality induction whether inter- or intramolecularly is clearly a pressing issue. Within the current literature on the subject of chirality generation (or chirogenesis) it is clear that the modes of chiral molecular communication are largely noncovalent in nature; primarily, attractive or repulsive electrostatic interactions (e.g., hydrogen bonding[6] and $\pi-\pi$[7] interactions) and repulsive steric interactions;[8] with these acting either independently or in collaboration to produce the observed chiral structures. Thus, it is with this in mind that we must approach the analyses of such dynamic supramolecular chiral systems.

Recently our and other research groups have been involved in applying the principles of supramolecular chirality induction to the development of smart functional porphyrin-based compounds, performing tasks such as absolute configuration determination, guest structure analysis, and molecular memory generation.[9,10a] In particular the bis(zinc porphyrin), **ZnZn**, Figure 1, has been found to be an exceptionally well-suited molecule for the application of supramolecular chirality induction principles, having been shown to function as an effective absolute configuration sensor, highly sensitive to factors such as ligand size, binding strength, stoichiometry, and composition as well as external influences such as temperature and phase transition.[9a,b,10a,c]

Although there are many aspects to the mechanism of the functioning of **ZnZn**, spectroscopic data, equilibria analysis, and interpretation by CPK molecular models lead us to the

* Corresponding authors. Phone: +81-6-6836-0063. Fax: +81-6-6836-1636 (V.V.B. and Y.I.). E-mail: victrb@inoue.jst.go.jp (V.V.B.) and inoue@chem.eng.osaka-u.ac.jp (Y.I.).

† ICORP, JST.

‡ Wako Pure Chemical Industries, Ltd.

10.1021/jp034300p CCC: $25.00
Published on Web 09/18/2003

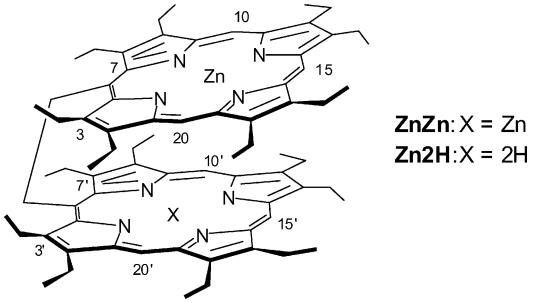

Figure 1. The structures (in syn form) of the porphyrin host molecules used in the study.

SCHEME 1: Schematic Representation of the Formation of the Left- and Right-Handed Screw Structures of ZnZn and Zn2H on Interaction with Enantiomeric Chiral Ligands

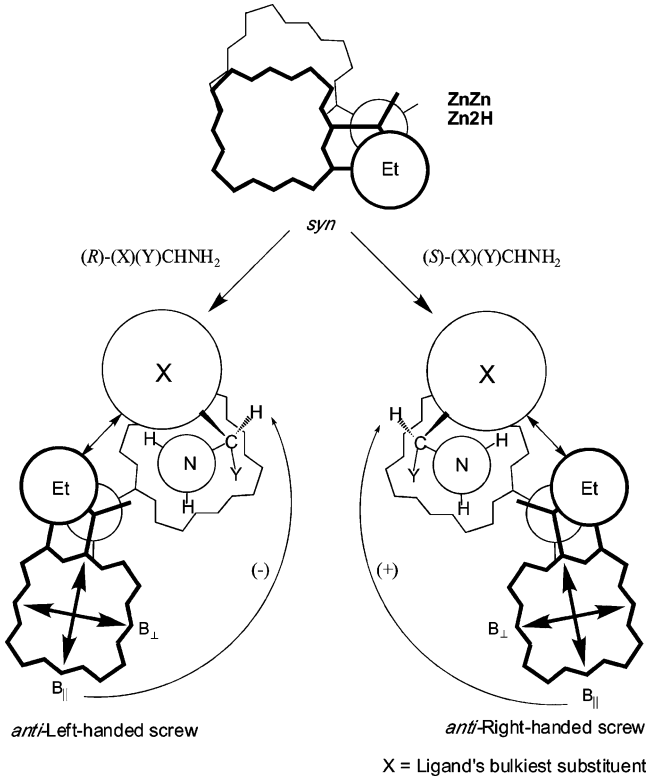

hypothesis that there are two key mechanistic points: first, syn−anti switching on ligation and second, steric repulsions between the chiral ligand's bulkiest substituent and the 3- and 7-ethyl groups of the neighboring porphyrin (Scheme 1).

It is the 3- and 7-ethyl groups in particular that are believed to be involved as the CPK model examination shows that other ethyl groups are too distant for any steric interaction. Further, such steric interactions can only occur if the second ligand coordination occurs from the inside face. If the coordination occurs from the outside face, then there is no possibility for steric interactions and consequently no supramolecular chirality induction (Scheme 2), although there may be point chirality contributions to the circular dichroism (CD) spectra. The result of this proposed mechanism, if the ligand is chiral, is the formation of an asymmetrical screw structure, from which the resulting CD spectrum allows the determination of the absolute configuration of the ligand (Scheme 1).[10a] Specifically, if the order of the bulkiness for the ligand's substituents corresponds with the priority rule, then *R* enantiomers induce negative (−) chirality and *S* enantiomers yield positive (+) chirality.

However, due to the dynamic nature of this host−guest system there are a number of possible conformations and stoichiometries. If the proposed mechanism based on ligand-ethyl group repulsion is active, only ligands coordinating in the inside manner allowing steric interactions will induce supramolecular chirality. This means that when two ligands are coordinated to **ZnZn** (as under the ligand excess conditions employed experimentally) three out of the four possibilities will be supramolecular chirally active (Scheme 3).

However, to-date, even after extensive efforts it has not been possible to show any direct observations of this mechanism, such as from X-ray or NOE analysis. To overcome this we have sought to obtain compelling indirect evidence of the functioning of this mechanism. To this end we have undertaken to study the effect of chiral ligand coordination to the monometalated zinc-freebase bis-porphyrin, **Zn2H** (Figure 1), which from a supramolecular chemistry point of view is a more simple case than **ZnZn**, having only one coordination site. It is postulated that, if our proposed mechanism is correct, then as only one molecule of ligand is able to bind to **Zn2H** (cf. two in **ZnZn**) only two bound species are possible, one inside (supramolecular chirally active) and one outside (supramolecular chirally inactive), Scheme 4.

Thus, the concentration of chiral species should be less than for **ZnZn**•L*$_2$ and thus the degree of chirality induction for a **Zn2H**•L* solution should be significantly less than that found for the corresponding **ZnZn**•L*$_2$ species.

Besides the mechanistic aspect, if this hypothesis is correct, **Zn2H** should be able to function as a new chirality sensor for compounds that **ZnZn** is unable to analyze. Particularly, it may be able to overcome a disadvantage of the **ZnZn** sensor, which possessing two binding sites, forms stable 1:1 tweezer host−guest complexes[11] resulting in significant difficulties in the evaluation of chiral bidentate compounds.

Experimental Section

Materials. The ethane-bridged bis-porphyrins, **ZnZn** and **Zn2H**, were synthesized according to the previously reported methods.[12] The chiral amines were purchased from Fluka Chemica AG and used as received. The amino acid derivatives shown in Figure 2 were purchased from Kokusan Chemical Works, Ltd.; Wako Pure Chemical Industries, Ltd.; and BACHEM AG as hydrochloride salts and were treated with NaOH in order to convert these salts into the corresponding free amines according to the previously reported procedure.[13] For CD and UV−vis measurements anhydrous CH_2Cl_2 was purchased from Aldrich Chemical Co., and CCl_4 (grade "infinity pure") was purchased from Wako Pure Chemical Industries, Ltd. and was used as received.

Spectroscopic Measurements. CD and UV−vis spectra were measured at room temperature on a JASCO J-720WI spectropolarimeter and Shimadzu UV-3101PC spectrometer, respectively. CD scanning conditions were as follows: scanning rate = 50 nm per min, bandwidth = 1 nm, response time = 0.5 s. The concentrations of the amines and amino acid derivatives used for the CD and UV−vis measurements were the concentrations where the spectral changes associated with the porphyrin chromophores were at their maximum, and any further increase in the concentrations of the amino acid derivatives had no effect on the signal intensities, positions, or profiles. ^{1}H NMR spectra were recorded at 400 MHz on a JEOL JNM-EX 400 spectrometer at various temperatures. Chemical shifts were referenced to the residual proton resonance of $CHCl_3$ (δ 7.25 ppm).

SCHEME 2: Schematic Representation of Supramolecular Chirogenesis in ZnZn Showing the Necessity for Inside Binding To Result in Chirality-Inducing Steric Interactions[a]

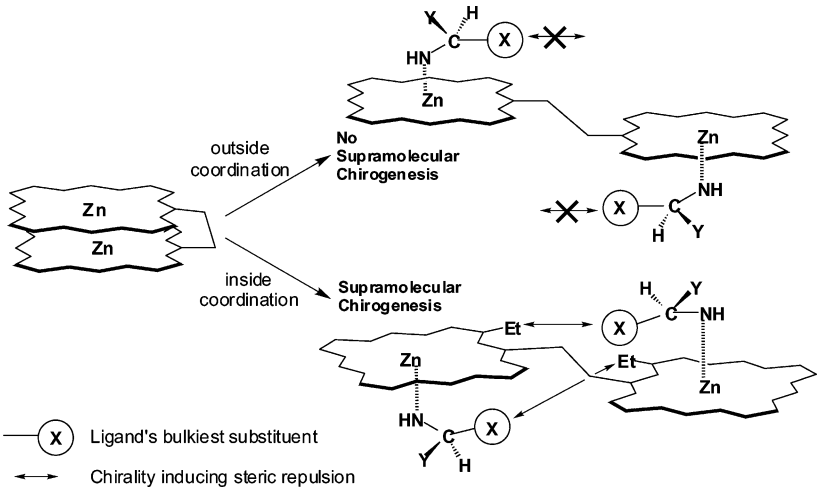

[a] Only the interacting ethyl groups are shown.

SCHEME 3: Schematic Representations of the Four Different Combinations of Inside and Outside Binding in ZnZn•L*$_2$[a]

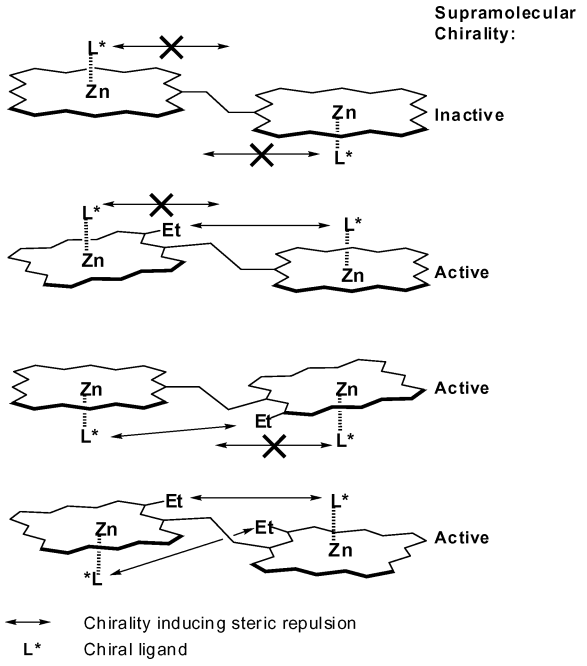

[a] Only the interacting ethyl groups are shown.

SCHEME 4: Schematic Representations of the Two Different Combinations of Inside and Outside Binding in Zn2H•L* [a]

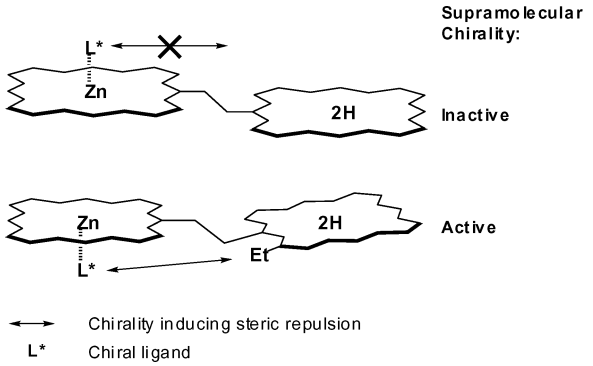

[a] Only the interacting ethyl groups are shown.

Results and Discussion

To investigate this hypothesis, that it is the steric repulsions between the chiral ligand's bulkiest substituent and the 3- and 7-ethyl groups of the neighboring porphyrin that result in supramolecular chirality induction, three enantiomeric pairs of amines belonging to the same homologue series, methyl esters of three L-amino acids, (*1R,2S*)-bornylamine, and (*1R,2R*)- and (*1S,2S*)-diaminocyclohexane were used as chirality-inducing ligands, Figure 2.

Absorption Spectral Changes. As discovered previously, initially both **ZnZn** and **Zn2H** at concentrations in the order of 10^{-6} M in dichloromethane are in the syn conformation due to $\pi-\pi$ interactions between the porphyrin macrocycles.[10b] This can be seen in Figure 3 from the almost identical $\lambda_{max}{}^{UV}$ values of the porphyrin Soret (B) bands in the UV−vis spectra of **ZnZn** and **Zn2H** of 397 and 399 nm, respectively. However, of note is the broader band of **Zn2H** in comparison to **ZnZn** (full width at half-maximum (fwhm) values of 54 and 31 nm, respectively). This arises from the presence of the two different chromophores in **Zn2H** and the weaker $\pi-\pi$ interactions due to the more ruffled nature of the freebase porphyrin macrocycle thus allowing greater conformational flexibility in **Zn2H**.

On addition of external ligands (concentrations in the order of $10^{-2}-10^{-1}$ M) dramatic changes are observed in the UV−vis spectra (see Tables 1−3 and Figure 3). As described previously[10a] the Soret band of **ZnZn** undergoes a red shift of approximately 30 nm to form a band with pronounced splitting (~10 nm) with the $\lambda_{max}{}^{UV}$ of the higher energy shifted band at around 425 nm, this arises from the ligand induced syn−anti conformational switching and amine coordination with the subsequent p_z-a_{2u} ligand-porphyrin orbital mixing[14] on the formation of **ZnZn**•L*$_2$. **Zn2H** undergoes similar but importantly different changes on formation of the anti **Zn2H**•L* species; the Soret band exhibits a similar red shift but is approximately 7 nm less so in comparison to **ZnZn**•L*$_2$'s lowest energy band. Further, it shows considerable broadening of the Soret band rather than any clear band splitting as observed previously in the interaction of **Zn2H** with achiral alcohols at low temperatures (that is as a result of different temperature regimes).[10b]

These observations are in good agreement with Kasha's exciton coupling theory,[15] thus corroborating the formation of

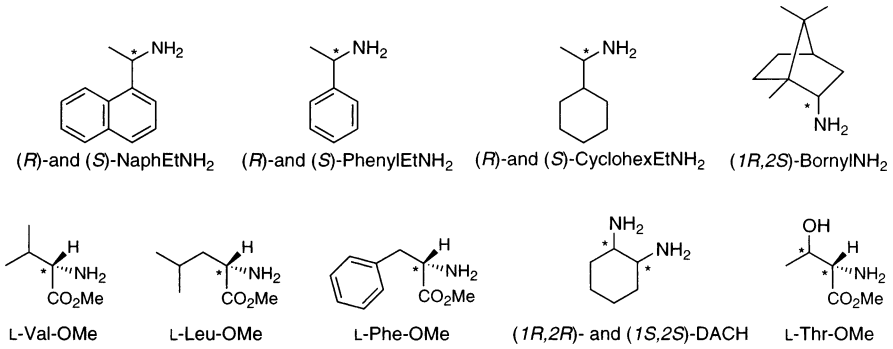

Figure 2. Ligands used for supramolecular chirality induction in the study.

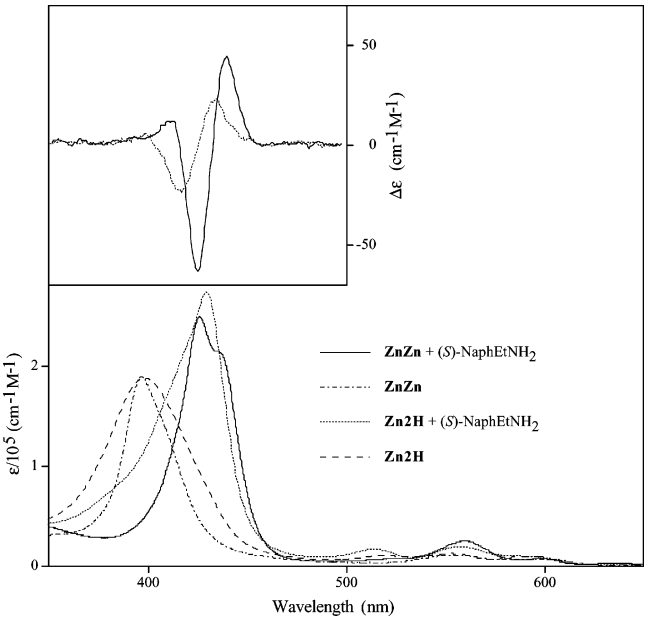

Figure 3. UV−vis and CD (inset) spectra of **ZnZn** and **Zn2H** with and without (*S*)-NaphEtNH$_2$ in CH_2Cl_2 at 293 K.

TABLE 1: Comparison of the fwhm Values of the ZnZn•L*$_2$ and Zn2H•L* Species in CH_2Cl_2 and CCl_4 Solvents at 293 K

	full width at half-maximum values (nm)		
ligand	**ZnZn** (CH_2Cl_2)	**Zn2H** (CH_2Cl_2)	**Zn2H** (CCl_4)
none[a]	31	54	52
(*R*)-NaphEtNH$_2$	33	38	62
(*S*)-NaphEtNH$_2$	33	38	63
(*R*)-1-PhenylEtNH$_2$	35	38	47
(*S*)-1-PhenylEtNH$_2$	35	38	47
(*R*)-1-CyclohexEtNH$_2$	35	37	46
(*S*)-1-CyclohexEtNH$_2$	35	36	46
(*S*)-1-BornylNH$_2$	33	35	47
L-Val-OMe	39	50	NA
L-Leu-OMe	39	48	75
L-Phe-OMe	36	42	75

[a] Without external ligands **ZnZn** and **Zn2H** are in the syn conformation.

the ligated anti conformations. As found for other porphyrin linear dimers and trimers,[16] the two degenerate $B_{||}$ and $B_{\perp}$ transitions (which are orientated either in a parallel or perpendicular direction relative to the connecting bridge axis) couple differently to produce the absorption band splitting in the UV−vis spectra, with transitions allowed only to the highest level of the $B_{\perp}$ states and the lowest level of the $B_{||}$ states in the case of an exactly parallel orientation of the porphyrin planes in dimeric structures. However, due to the screw structure formed in **ZnZn**•L*$_2$ all eight possible transitions are allowed, with the major contributions from the above-mentioned pairs ($B_{||}$ and $B_{\perp}$) of the coupled electric dipoles.[10a] In the case of **Zn2H**•L* the presence of two different porphyrin rings means that the transitions of each ring are now nondegenerate; further, the presence of only one ligand results in a more flexible conformation than the **ZnZn**•L*$_2$ species at room temperature due to the steric hindrance contribution from only one ligand. The combination of these two factors is the predominant reason for the broader and nonsplit band of **Zn2H**•L*, while for achiral alcohols at low temperatures the decreasing conformational flexibility results in the narrowing and more pronounced splitting of the Soret band.[10b] Indeed, the comparative broadness of the Soret bands of the **ZnZn**•L*$_2$ and **Zn2H**•L* species (evaluated by their fwhm values) allows a handle to be gained on the relative magnitudes of the steric effects exerted in each. As can be seen in Table 1 (the left and middle columns), the fwhm values of the **ZnZn**•L*$_2$ species are all significantly smaller than the equivalent **Zn2H**•L* species, showing that overall the **ZnZn**•L*$_2$ in solution is more conformationally rigid. This is due to the presence of the higher percentage of species with the flexibility reducing chiral steric repulsions (**ZnZn**•L*$_2$ 75% and **Zn2H**•L* 50%) as well as the "two ligands−two steric contributions" species (Scheme 3) that cannot occur in the **Zn2H**•L* case, overall resulting in a more flexible species.

Although as described before the red shifted **Zn2H**•L* Soret band is also indicative of an anti structure, the lesser degree of this shift is expected due to the following reason. In comparison to the two **Zn**•L* moieties of **ZnZn**•L*$_2$ which are of equal energy, the **Zn**L* and **2H** moieties of **Zn2H**•L* significantly differ in the energy of the B electronic transition, based on the monomeric porphyrins (with the freebase moiety being higher as ligand coordination lowers the energy of the B transition considerably[14a]), thus the effect of the exciton coupling of the two chromophores of higher and lower energies in anti **Zn2H**•L* is to result in an overall blue shift in the B transitions relative to **ZnZn**•L*$_2$ which has two chromophores of lower and equal energy. Thus the above UV−vis observations, which apply to all the ligands studied, correlate well with proposed mechanism of syn−anti switching and ligand-ethyl group steric repulsion as was observed in the case of achiral alcohols.[10b]

Circular Dichroism Spectral Changes. Bearing in mind the spectral changes observed in the UV−vis spectra, the CD properties of these systems were investigated. Monitoring and comparison of the CD spectral changes of **ZnZn** and **Zn2H** on the addition of the enantiopure ligands revealed dramatic insights into the mechanism of the chirality induction in these systems. In the case of **ZnZn** detailed analysis of the CD spectral changes has been previously carried out.[10a,c,13,17] Specifically, addition of the chiral ligands to achiral **ZnZn**, which is inherently CD

TABLE 2: UV−vis and CD Spectral Data of ZnZn Interacting with Different Ligands at 293 K

ligand	UV−vis data λ^{UV} (nm) [$\epsilon/10^5$ (M^{-1} cm^{-1})] split Soret	UV−vis data λ^{UV} (nm) [$\epsilon/10^5$ (M^{-1} cm^{-1})] band maxima	CD data λ^{CD} (nm) [$\Delta\epsilon_n$ (M^{-1} cm^{-1})] first Cotton ($n = 1$) effect	CD data λ^{CD} (nm) [$\Delta\epsilon_n$ (M^{-1} cm^{-1})] second Cotton ($n = 2$) effect	*A* value[a]
(*R*)-NaphEtNH$_2$	436 [2.12]	426 [2.35]	439 [−51.2]	426 [+56.7]	−107.9
(*S*)-NaphEtNH$_2$	436 [2.14]	426 [2.50]	439 [+44.5]	426 [−63.2]	+107.7
(*R*)-PhenylEtNH$_2$	436 [2.11]	426 [2.26]	439 [−42.0]	425 [+42.1]	−84.1
(*S*)-PhenylEtNH$_2$	436 [2.12]	426 [2.35]	439 [+33.7]	425 [−44.7]	+78.4
(*R*)-CyclohexEtNH$_2$	438 [2.53]	427 [2.52]	439 [−33.1]	425 [+39.6]	−72.7
(*S*)-CyclohexEtNH$_2$	438 [2.46]	427 [2.46]	439 [+31.7]	425 [−36.1]	+67.8
(*S*)-BornylNH$_2$	437 [2.54]	427 [2.81]	439 [+54.8]	425 [−74.9]	+129.7
L-Val-OMe	437 [2.69]	425 [2.71]	438 [+13.9]	425 [−20.3]	+34.2
L-Leu-OMe	436 [2.72]	426 [2.78]	438 [−23.0]	424 [+26.7]	−49.7
L-Phe-OMe	436 [2.94]	425 [2.96]	438 [−84.3]	423 [+86.3]	−170.6

[a] $A = \Delta\epsilon_1 - \Delta\epsilon_2$; this represents the total amplitude of the CD couplet. The difference in sign of the L-amino acids is due to the difference in relative bulkiness of the substituents at the chiral center in relation to the priority rule (see ref 13). CH_2Cl_2 solvent.

TABLE 3: UV−vis and CD Spectral Data of Zn2H Interacting with Different Ligands at 293 K

ligand	UV−vis data λ^{UV} (nm) [$\epsilon/10^5$ (M^{-1} cm^{-1})] Soret band maxima	CD data λ^{CD} (nm) [$\Delta\epsilon_n$ (M^{-1} cm^{-1})] first Cotton ($n = 1$) effect	CD data λ^{CD} (nm) [$\Delta\epsilon_n$ (M^{-1} cm^{-1})] second Cotton ($n = 2$) effect	*A* value[a]	% reduction[b]
(*R*)-NaphEtNH$_2$	430 [2.75]	432 [−23.2]	418 [+23.6]	−46.8	56.6
(*S*)-NaphtEtNH$_2$	430 [2.76]	435 [+23.2]	417 [−22.4]	+45.6	57.7
(*R*)-PhenylEtNH$_2$	429 [2.70]	437 [−16.6]	418 [+14.8]	−31.4	62.7
(*S*)-PhenylEtNH$_2$	429 [2.68]	434 [+16.3]	418 [−19.8]	+36.1	54.0
(*R*)-CyclohexEtNH$_2$	429 [2.74]	436 [−13.6]	414 [+13.8]	−27.4	62.3
(*S*)-CyclohexEtNH$_2$	430 [2.74]	433 [+9.7]	420 [−17.1]	+26.8	60.5
(*S*)-BomylNH$_2$	430 [2.97]	434 [+20.3]	418 [−27.7]	+48.0	63.0
L-Val-OMe	428 [2.21]	430 [+4.3]	415 [−6.2]	+10.5	69.3
L-Leu-OMe	428 [2.30]	433 [−7.3]	418 [+8.3]	−15.6	68.6
L-Phe-OMe	429 [2.48]	432 [−26.8]	417 [+20.7]	−47.5	72.2

[a] $A = \Delta\epsilon_1 - \Delta\epsilon_2$, this represents the total amplitude of the CD couplet. CH_2Cl_2 solvent. The difference in sign of the L-amino acids is due to the difference in relative bulkiness of the substituents at the chiral center in relation to the priority rule (see ref 13). [b] Reduction of the **Zn2H•**L* *A* values compared to the equivalent **ZnZn•**L*$_2$ species. CH_2Cl_2 solvent.

inactive, results in the appearance of bisignated Cotton effects whose λ^{CD} values correspond well with the λ^{UV} values of the split Soret band in the UV−vis spectra, Figure 3, Table 2.[10a,c,13,17] The order of the signs of these first and second Cotton effects has been shown to be a powerful tool for the determination of the absolute configuration of numerous chiral compounds and the relative sizes of substituent groups.[10a,c,13,17]

In these **ZnZn•**L*$_2$ species the chirality occurs, as depicted in Schemes 1 and 2, from the steric interaction between the ligand's most bulky substituent and the **ZnZn**'s ethyl groups at the 3- and 7-positions when the ligand is coordinated from the inside face. From the dynamics of the various possible species shown in Scheme 3, it can be seen that three out of the four species are supramolecularly chiral; with one having two steric contributions (inside−inside) and two one contribution (inside−outside and outside−inside). However, thus far it has not been possible to experimentally determine the different degree of chirality induction made by the bis-ligated (inside−inside) species compared to the bis-ligated (inside−outside and outside−inside) species.

The CD λ^{CD} and *A* values of the **Zn2H•**L* species are, however, in dramatic contrast to the **ZnZn•**L*$_2$ species and provide revealing insights into the supramolecular chirality induction mechanism, Table 3.

Initially, it is clear from Table 3 and Figure 3 that the λ^{CD} of the Cotton effects of the **Zn2H•**L* species are blue shifted in comparison to the corresponding **ZnZn•**L*$_2$ species, which shows, as expected, that they arise from the same B band transitions that are also blue shifted in the UV−vis spectra as discussed above.

Additional proof for this high energy shift of the B transitions upon the formation of the chiral anti **Zn2H•**L* species is obtained from theoretical calculations, using a nonlinear least-squares method developed for the analysis of multistep equilibria.[18] Applying this method to the **ZnZn**-to-**ZnZn•**L*$_2$ case, it was possible to calculate the theoretical UV−vis and CD spectra of the intermediate anti **ZnZn•**L* species,[9a] which is clearly very similar to the anti **Zn2H•**L* species considered here, and as such the two should possess very similar spectral properties. The theoretical UV−vis and CD spectra of **ZnZn•**L and the experimental **Zn2H•**L* are shown in Figure 4.

Although there are differences between the theoretical and experimental spectra, which is to be expected due to the different chromophores (**Zn** and **2H** subunits), they are very well matched in both position and profile, additionally confirming the nature of the **Zn2H•**L* species. Further, these data also support the model used here for coupling between the **Zn** and **2H** chromophores. In comparison to the **ZnZn•**L*$_2$ species the absorbance maximum and the first Cotton effect of **ZnZn•**L* is blue shifted by (12 nm). This is because in the **ZnZn•**L* species the unligated moiety is higher in energy than the ligated moiety, resulting in an increase in the energy of the excited state of the coupled chromophores. This situation is very close to that observed for **Zn2H•**L*, where the **2H** species is higher in energy resulting in a similar elevation in energy.

Critically, however, the intensities of the Cotton effects of **Zn2H•**L* (as typified by the *A* values) are dramatically reduced in comparison to **ZnZn•**L*$_2$. The magnitude of the reduction ranges from 57% for the (*R*)-NaphEtNH$_2$ complexes to 72% for the L-Phe-OMe complexes, with an average overall reduction

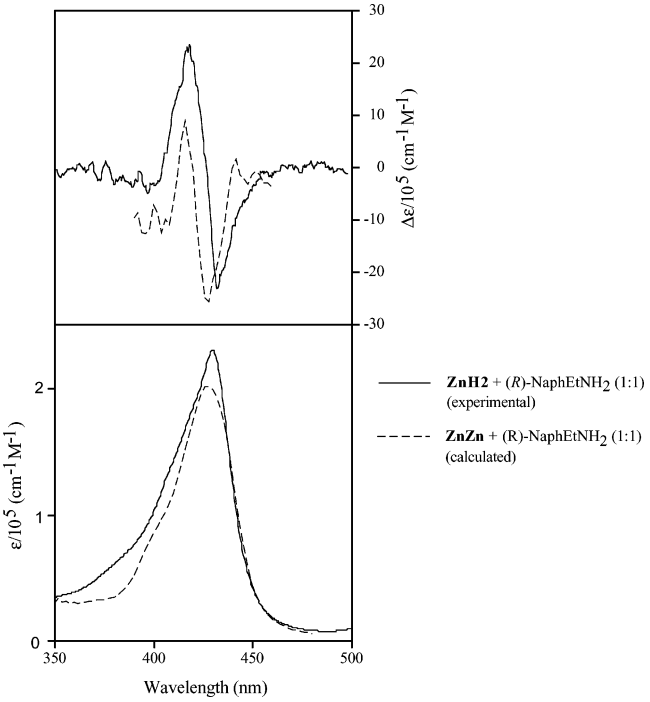

Figure 4. UV−vis and CD spectra of the calculated spectra of **ZnZn**+(*R*)-NaphEtNH$_2$ (1:1) and the experimental spectra **Zn2H**+(*R*)-NaphEtNH$_2$ (1:1).

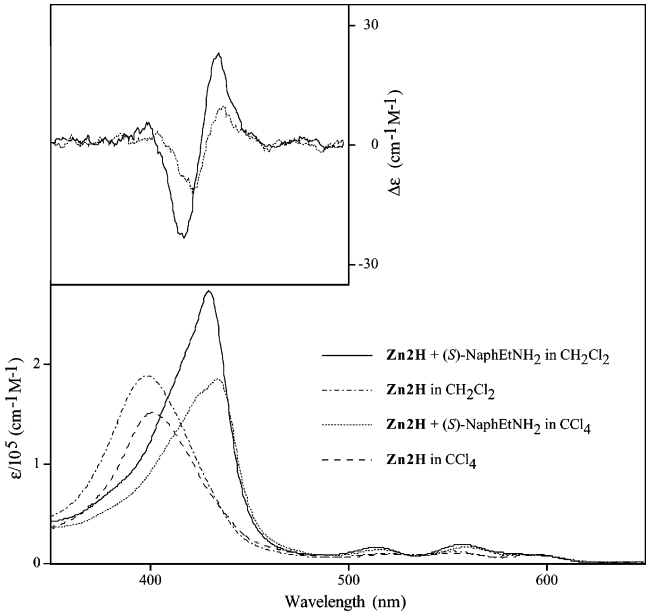

Figure 5. UV−vis and CD (inset) spectra of **Zn2H** with and without (*S*)-NaphEtNH$_2$ in CH_2Cl_2 and CCl_4 at 293 K.

of 63% for all 10 complexes studied. A qualitative analysis of this highlights the nature of the chirality induction mechanism, assuming equivalent binding constants for inside and outside coordination. In the proposed chirality induction mechanism there are two major components that contribute to the magnitude of the observed chirality: (1) the number of chirally active species and (2) the number of chirality-inducing steric interactions (see Schemes 3 and 4). In the case of **ZnZn**•L*$_2$ there are three supramolecularly chirally active species out of four possibilities, and for **Zn2H**•L* there is one out of two possibilities. If it is assumed that both the complexes (with either one or two supramolecularly active steric interactions) produce the same degree of chirality, then we should expect that the **Zn2H**•L* complexes would have an *A* value reduction of about 33%. However, the observed average, as stated, is 63%. Thus it may be assumed that it is the total number of supramolecularly chirality-inducing steric interactions that are responsible for the overall observed magnitude of chirality induction, with the **ZnZn**•L*$_2$ species having four such steric interactions, while **Zn2H**•L* has but one. In this context we should expect a reduction of around 75% in the degree of chirality, which is indeed closer to the 63% observed (some deviation is expected due to the structural and chromophoric differences between the freebase and zinc porphyrin systems as well as from the contribution of the point chirality effect observed upon ligation of chiral amines[10a]). While this is a qualitative analysis, it clearly shows that it is the number of chiral steric interactions between the ligand's bulkiest substituents and the neighboring porphyrin's 3- and 7-ethyl groups that gives rise to the observed induced chirality and, to an extent, accounts for the relative magnitudes. That is, as previously experimentally shown, bulkier substituents are able to exert larger steric interactions and thus generate a greater degree of chirality.[13,17]

Solvent Effect on the Chirality Induction Mechanism. To further investigate the factors affecting this mechanism, the chiroptical properties of the chirality induction observed for **Zn2H**•L* in nonpolar CCl_4 were investigated (CCl_4 was selected as the nonpolar and noncoordinating equivalent of CH_2Cl_2). As can be seen from Figure 5 with the appearance of the bisignate Cotton effects on addition of the chiral ligand, the same basic form of chirality induction is operating in both solvents. The results for the 10 studied ligands are shown in Tables 4 and 5 and are compared to the results for CH_2Cl_2 shown in Table 3.

The essential observations are as follows. Both the UV−vis absorption maxima and Cotton effects of the bound species in CCl_4 are moderately red shifted by approximately 5 nm, apparently due to the lower solvation effect resulting in enhanced binding of the amine and subsequent enhancement of the ligand−porphyrin orbital mixing. More importantly, the magnitudes of the Cotton effects are dramatically reduced in comparison to the corresponding complexes in CH_2Cl_2. Indeed, the *A* values for the complexes in CCl_4 were reduced by an average of 45%. From the analysis of these data it is believed that this is due to the different solvent−complex interactions. In all cases the chirality is enhanced in CH_2Cl_2 because this solvent is more polar than CCl_4 and can interact with the ligand's and porphyrin's substituents to a greater extent, thus increasing their corresponding effective sizes; resulting in larger chiral steric interactions and hence a greater degree of chirality induction, in comparison to CCl_4 which is not able to enhance the substituent's bulkiness to the same extent.

There are two major issues regarding the nature of the studied ligands and how the solvent effects them: (1) In the case of the homologue series NaphEtNH$_2$, PhenylEtNH$_2$ and CyclohexNH$_2$ the Me group is small in comparison to the bulkiest substituent and will be substantially less affected by solvent interactions, thus it is possible to consider the effect of the solvent solely on the largest group. (2) The bulkiest substituents are chosen to see how their electrostatic nature affects the interaction with the solvent. Thus the quadrupolar nature of the aromatic substituents in NaphEtNH$_2$, phenylEtNH$_2$, and L-Phe-OMe are able to electrostatically interact, to a greater extent, than the substantially less polar alkyl groups. Thus, it is judicious to compare the phenylEtNH$_2$ and CyclohexEtNH$_2$ ligands as these are aromatic and alkyl analogues, respectively.

Initially it can be seen that the fwhm values in CCl_4 in Table 1 are all substantially larger than those for the complexes in CH_2Cl_2, showing that the complexes' conformational flexibili-

TABLE 4: UV−Vis and CD Spectral Data of the System Zn2H Interacting with Different Ligands in CCl_4 at 293 K

ligand	UV−vis data λ^{UV} (nm) [$\epsilon/10^5$ M^{-1} cm^{-1})] Soret band maxima	CD data λ^{CD} (nm) [$\Delta\epsilon_n$ (M^{-1} cm^{-1})] first Cotton ($n = 1$) effect	CD data λ^{CD} (nm) [$\Delta\epsilon_n$ (M^{-1} cm^{-1})] second Cotton ($n = 2$) effect	*A* value[a]	% reduction[b]
(*R*)-NaphtEtNH$_2$	435 [1.83]	435 [−10.3]	420 [+12.3]	−22.6	51.7
(*S*)-NaphEtNH$_2$	435 [1.86]	438 [+9.7]	422 [−12.0]	+21.7	52.4
(*R*)-PhenylEtNH$_2$	434 [2.17]	433 [−2.3]	418 [+10.5]	−12.8	59.2
(*S*)-PhenylEtNH$_2$	434 [2.17]	437 [+9.5]	423 [−5.6]	+15.1	58.2
(*R*)-CyclohexEtNH$_2$	434 [2.20]	437 [−6.7]	420 [+11.9]	−18.6	32.1
(*S*)-CyclohexEtNH$_2$	434 [2.20]	436 [+11.9]	423 [−5.3]	+17.1	36.2
(*S*)-BornylNH$_2$	434 [2.11]	439 [+16.6]	422 [−8.1]	+24.7	48.5
L-Val-OMe	432 [1.86]	438 [+3.5]	419 [−2.3]	+5.8	44.8
L-Leu-OMe	433 [1.64]	436 [−2.9]	420 [+8.2]	−11.1	28.8
L-Phe-OMe	434 [1.63]	437 [−16.0]	423 [+15.0]	−31.0	34.7

[a] $A = \Delta\epsilon_1 - \Delta\epsilon_2$, this represents the total amplitude of the CD couplet. The difference in sign of the L-amino acids is due to the difference in relative bulkiness of the substituents at the chiral center in relation to the priority rule (see ref 13). [b] Reduction of the **Zn2H•**L* *A* values in CCl_4 compared to the **Zn2H•**L* values in CH_2Cl_2.

TABLE 5: *g* Factor Data of Zn2H Interacting with Different Ligands in CH_2Cl_2 and CCl_4 at 293 K

ligand	*g* factor amplitude[a,b] (10^{-5}) CH_2Cl_2	*g* factor amplitude[a,b] (10^{-5}) CCl_4	% reduction[c]
(*R*)-NaphEtNH$_2$	−21	−14	33
(*S*)-NaphEtNH$_2$	+21	+12	43
(*R*)-PhenylEtNH$_2$	−17	−7	59
(*S*)-PhenylEtNH$_2$	+17	+8	53
(*R*)-CyclohexEtNH$_2$	−15	−10	33
(*S*)-CyclohexEtNH$_2$	+12	+9	25
(*S*)-BomylNH$_2$	+25	−18	28
L-Phe-OMe	−22	−19	14
L-Val-OMe	NA	NA	NA
L-Leu-OMe	NA	NA	NA

[a] The *g* factor amplitude is the total amplitude of the *g* factor in the region corresponding to the Cotton effects in the CD spectra. [b] The accuracy of the *g* factor amplitude values is $\pm 2 \times 10^{-5}$ as determined from baseline evaluation. [c] Reduction of the **Zn2H•**L* *g* factor amplitude values in CCl_4 compared to the equivalent **Zn2H•**L* values in CH_2Cl_2.

ties, and thus the magnitudes of their steric interactions, for the **Zn2H•**L* in CCl_4 complexes are much smaller than for the **Zn2H•**L* in CH_2Cl_2 cases. This is due to the fact that, regardless of substituent, CH_2Cl_2's dipole allows it to interact with the ligand's substituents in a way that CCl_4 cannot, thus increasing their effective size—consequently reducing the conformational freedom in the supramolecular complex, and thus resulting in lower fwhm values. To further and more accurately assess this supposition, analysis of the anisotropy (*g*) factor ($g = \Delta\epsilon/\epsilon$) amplitude was undertaken (Table 5), as this is the true measure of the induced chirality of the system, being independent of other factors influencing the light absorption processes.

Comparing the analogous PhenylEtNH$_2$ and CyclohexEtNH$_2$ ligands it is revealed that the reduction in the average *g* factor for PhenylEtNH$_2$ is 56%, whereas it is 29% for CyclohexEtNH$_2$. This clearly illustrates that the quadrupolar aromatic phenyl EtNH$_2$ is much more able to interact with the polar CH_2Cl_2 than the alkyl CyclohexEtNH$_2$, resulting in a significant reduction in its effective size and consequently a larger reduction in the *g* factor in CCl_4 (with which it is less able to interact) than for CyclohexEtNH$_2$. The lower ability of the alkyl substituents to interact with CH_2Cl_2 is further seen in the case of BornylNH$_2$ with a reduction of only 28%.

Analysis of the NaphEtNH$_2$ and L-Phe-OMe cases also reveals the presence of the same effect. In the case of NaphEtNH$_2$ its reduction is smaller than that of phenylEtNH$_2$. This is believed to be because the naphthyl group is large enough that the change

SCHEME 5: Schematic Representation of the Solvent Effect on Supramolecular Chirality Induction in Zn2H•L*

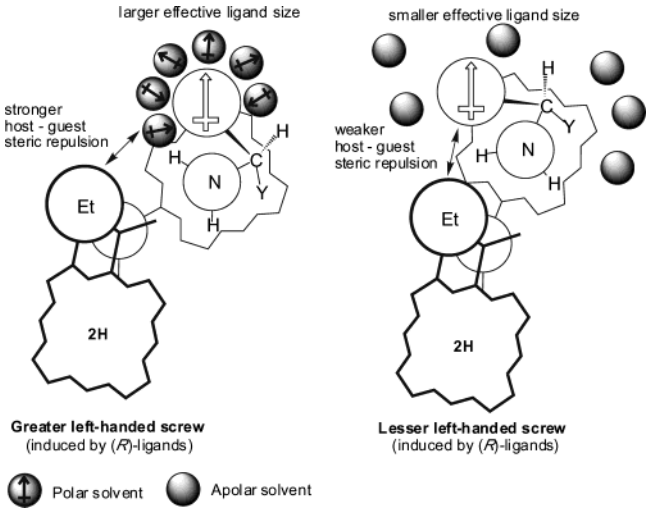

in effective size caused by the different level of interaction with the two solvents is small compared to the size of the naphthyl group, resulting in the smaller percentage change in the *g* factor. For L-Phe-OMe both the Phe and CO_2Me moieties are polar and are thus able to interact with CH_2Cl_2 at a similar level. Consequently they are also affected in a similar way (reduction in effective size) by the change in solvent to CCl_4, resulting in only a relatively small percentage change in induced chirality. In summary the effect of the different solvents can be illustrated schematically as shown in Scheme 5.

Application of Zn2H as a New Chirality Sensor for Bidentate Ligands. An additional important sensing property of **Zn2H** was found in the course of our study. Previously **ZnZn** has been shown to perform as an excellent sensor for the absolute configuration determination of a variety of ligands such as monoalkyl/aromatic amines, monoalkyl/aromatic alcohols, and amino acid derivatives.[10c,13,17] However, there is one particular group of molecules for which serious problems occur, often leading to an inability to determine the absolute configuration, namely bidentate compounds such as diamines and amino alcohols. In this case the formation of a 1:1 tweezer complex,[11] in which the ligand is bound between the two zinc porphyrins by the coordination of each functional group to a different zinc ion, prevents the determination of the absolute configuration. This was observed for enantiopure 1,2-diphenylethylenediamine, but, in this case, the problem could be

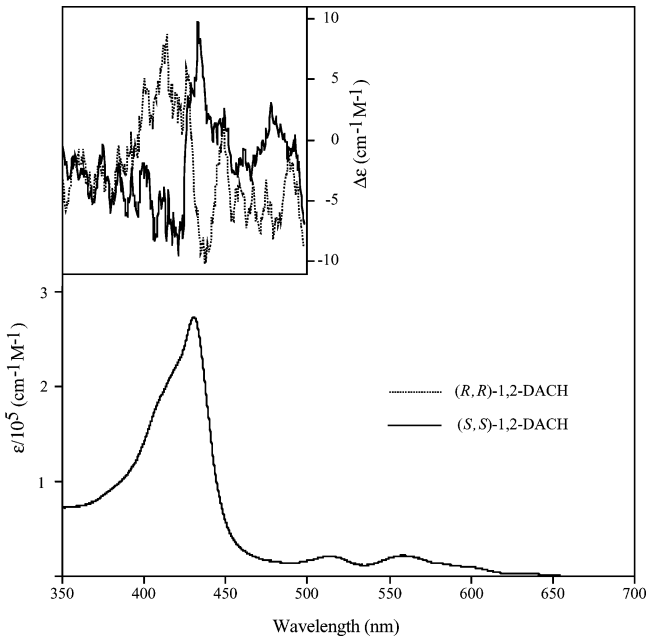

Figure 6. UV−vis and CD (inset) spectra of **Zn2H** with (*R*,*R*)- and (*S*,*S*)-1,2-DACH in CH_2Cl_2 at 293 K.

overcome by increasing the concentration of the ligand to such an extent so to force the formation of the conventional 1:2 complex from which the absolute configuration could be determined.[11a] However in the case of 1,2-diaminocyclohexane (1,2-DACH) the 1:1 complex was so strong ($K > 10^7$ M^{-1}) that the 1:2 complex could not be formed under any conditions.[11b] However if the complex between **Zn2H** and 1,2-DACH is allowed to form then because there is only one coordination site at the zinc porphyrin, and as the **Zn2H** concentration is very low ($\sim 1 \times 10^{-6}$ M) only the conventional anti **Zn2H•**L* complex can form, Figure 6.

The changes in the UV−vis spectra, as seen previously for the other ligands, show the formation of the anti **Zn2H•**L* complex. Further and in accordance with previous results and the proposed mechanism of supramolecular chirality induction,[10a,13,17] the CD spectra show that the ligand's absolute configurations can be read out despite the low intensity of the induced CD signals which arise from the small difference in effective size between the C(H) and C(NH) substituents of the asymmetric carbons of 1,2-diaminocyclohexane. Thus the (*R*,*R*) enantiomer induces negative first and positive second Cotton effect, and the (*S*,*S*) enantiomer induces positive first and negative Cotton effect. Thus in this case application of the single site coordination properties of **Zn2H** has overcome a previously insurmountable problem. A further example of the advantage of **Zn2H** for overcoming such problems is in the absolute configuration determination of the bis-functional amino acid derivative L-Thr-OMe. When **ZnZn** is applied to this end the determination is complicated as a result of the formation of a 1:1 tweezer complex of opposite (negative) chirality.[19] The application of the **Zn2H** and the subsequent single site binding, however, results in the correct (positive) chirality and thus the elucidation of the absolute configuration.

As an additional and unambiguous proof of the formation of the chiral anti **Zn2H•**L* complex a variable temperature (VT) ^{1}H NMR study[20] was carried out, with the resulting spectra shown in Figure 7.

From the initial spectrum (a) it is clear that free **Zn2H** is in the achiral syn conformation, with the signals of the 10,20-meso protons of each porphyrin ring (**Zn** and **2H**) existing as

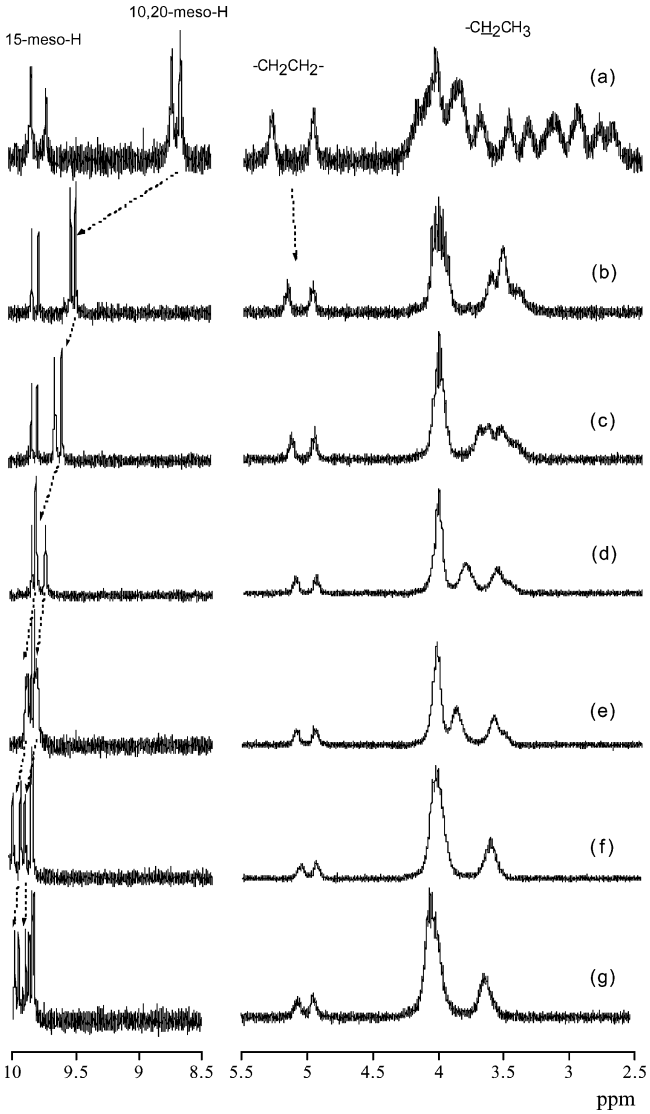

Figure 7. Temperature induced changes in the ^{1}H NMR spectrum of **Zn2H** at 293 K (a) and of the **Zn2H** (*S*,*S*)-1,2-DACH complex (molar ratio 1:5) in $CDCl_3$ upon cooling at temperatures 328 K (b), 318 K (c), 303 K (d), 293 K (e), 283 K (f), and 273 K (g).

singlets of two protons each (8.80 and 8.73 ppm), showing that they are in identical magnetic environments. Furthermore, the methylene protons of the ethyl groups exist, as expected, as several independent signals which are indicative of the syn conformation, as previously shown for both the single bonded bridged syn **ZnZn**[10b] and the *cis*-ethene-bridged equivalent of **ZnZn**.[21] On addition of 5 equiv of enantiopure (*S*,*S*)-1,2-DACH **Zn2H** undergoes dramatic conformational changes which can be well rationalized by considering the effect of temperature on the constant concentration sample, Figure 7(b)−(g). In comparison with the room-temperature ligand free sample (a), for **Zn2H•**L* at 328 K (b) the 10,20-meso protons have undergone large downfield shifts of $\Delta\delta$ 0.75 and 0.78 ppm, a process which continues on further temperature reduction resulting in $\Delta\delta$'s of 1.01 ppm for both the 10,20-meso protons at 303 K. Importantly though the 10,20-meso protons still remain as two singlets. These spectral changes show that while the **Zn2H•**L* complex forms and, with decreasing temperature, the percentage bound increases and the anti conformation is progressively more adopted, the whole complex is still supramolecularly achiral on the NMR time scale at these temperatures. This is due to the still high conformational flexibility

of the **Zn2H•**L* complex that essentially results in (NMR time scale) thermal racemization of the supramolecular chirality. However on subsequent temperature reductions, (e)−(g), the percentage bound further increases (increasing the number of chirality-inducing steric interactions), and the thermally induced conformational flexibility is further diminished (reducing the degree of thermal racemization). These changes result in further downfield shifting of the 10,20-meso protons as the syn-to-anti conversion progresses and more importantly the splitting of these two signals into four one-proton signals. This shows that each proton is in an independent magnetic environment, which arises directly from the formation of the supramolecular chiral screw structure of anti **Zn2H•**L*. Also, as the temperature is reduced dramatic changes are observed in the region of the ethyl group methylene protons. The "fingerprint" multiplet signals of syn **Zn2H** are rapidly lost on addition of (*S*,*S*)-1,2-DACH at 328 K resulting in two broad signals (3.61 and 3.84 ppm), and on further cooling to 303 K the more upfield signal splits into two; this arises because the more pronounced screw structure brings four of the ethylene groups into a more deshielded region resulting in the observed downfield shift. This process continues until two broad multiplets of ratio 3:1 are formed, as seen previously in the aforementioned single bonded bridged anti **ZnZn**[10b] and the double bonded bridged trans alkene equivalent of **ZnZn**.[10b,21] Of note, the 15-meso and $-CH_2CH_2-$ bridge protons are largely unaffected by these structural changes as observed in the case of other titration and VT experiments on **ZnZn**.[9a,10c] Thus from these experiments we can see the clear formation of the **Zn2H•**L* species and on temperature reduction follow the progressive syn−anti conversion and the adoption of the supramolecular chiral screw conformation.

Conclusion

The rationalization of the chirality induction mechanism operating in such a sensitive system as that studied here is crucial if the results are to be correctly understood and applied. In this case the key issue is does the evidence from the above experiments support the proposal that it is the steric interactions between the ligand's bulkiest substituent and the host's 3- and 7-ethyl groups, when the ligand is inside coordinated, that are responsible for the induction and magnitude of the observed chirality.

From the changes in the UV−vis spectra on ligand coordination, and their correlation with exiton coupling theory as well as ^{1}H NMR data, it can be clearly seen that the **Zn2H•**L* species adopts the anti conformation in the manner of the **ZnZn•**L*$_2$ analogue. Further, the relative conformational flexibilities show a clear dependence on the bulk of the ligand (and thus the degree of steric hindrance). Analysis of the CD data clearly shows that the induced chirality is dramatically reduced in the **Zn2H•**L* system, with the critical factor affecting the magnitude found not to be the number of chiral species but indeed the number of supramolecular chirality-inducing steric interactions. Additionally, the same chirality-inducing steric mechanism can also found to be involved in the lower degree of chirality induction observed for the **Zn2H•**L* system in CCl_4 rather than CH_2Cl_2. In this case the lower ability of the CCl_4 to electrostatically interact with the ligand and porphyrin reduces the corresponding effective size of the substituents thus reducing the degree of steric repulsion between the bulkiest ligand substituent and the neighboring porphyrin's 3- and 7-ethyl groups. Finally, whereas in our previous work we have applied **ZnZn•**L*$_2$ compounds for the determination of absolute configurations and the analysis of guest structures, we see here that indeed only a single coordination point is in fact necessary for these tasks and is able to overcome previous absolute configuration determination problems. However, it is clear that to optimize the sensitivity of such molecular devices, the number of coordination points (i.e. use of **ZnZn•**L*$_2$) and the number of supramolecular chirality-inducing steric interactions should be maximized as well as maximized and judicious choices should be made in external aspects (in this case solvent use) in order to enhance the system's desired properties.

References and Notes

(1) (a) Schmitzer, A. R.; Franceschi, S.; Perez, E.; Rico-Lattes, I.; Lattes, A.; Thion, L.; Erard, M.; Vidal, C. *J. Am. Chem. Soc*. **2001**, *123*, 5956−5961. (b) Lee, D. H.; Granja, J. R.; Martinez, J. A.; Severin, K.; Ghadiri, M. R. *Nature* **1996**, *382*, 525−528. (c) Montanari, F.; Casella, L. *Metalloporphyrin Catalyzed Oxidation*; Kluwer: Dordrecht, 1994.

(2) (a) Lin, W.; Wang, Z.; Ma, L. *J. Am. Chem. Soc*. **1999**, *121*, 11249−11250. (b) Verbiest, T.; Van Elshocht, S.; Kauranen, M.; Hellemans, L.; Snauwaert, J.; Nuckolls, C.; Katz, T. J.; Persoons, A. *Science* **1998**, *282*, 913−915.

(3) (a) Lorenzo, M. O.; Baddeley, C. J.; Muryn, C.; Raval, R. *Nature* **2000**, *404*, 376−379. (b) Akagi, K.; Piao, G.; Kaneko, S.; Sakamaki, K.; Shirakawa, H.; Kyotani, M. *Science* **1998**, *282*, 1683−1686. (c) Jung, J. H.; Ono, Y.; Shinkai, S. *Angew. Chem., Int. Ed*. **2000**, *39*, 1862−1865. (d) Kepert, C. J.; Prior, T. J.; Rosseinsky, M. J. *J. Am. Chem. Soc*. **2000**, *122*, 5158−5168.

(4) (a) Feringa, B. L.; van Deldon R. A.; Koumura, N.; Geertsema, E. M. *Chem. Rev*. **2000**, *100*, 1789−1816. (b) Fujiki, M.; Koe, J. R.; Motonaga, M.; Nakashima, H.; Terao, K.; Teramoto, A. *J. Am. Chem. Soc*. **2001**, *123*, 6253−6261. (c) Koumura, N.; Zijlstra, R. W. J.; van Deldon, R. A.; Harada, N.; Feringa, B. L. *Nature* **1999**, *401*, 152−155.

(5) (a) Tashiro, K.; Konishi, K.; Aida, T. *J. Am. Chem. Soc*. **2000**, *122*, 7921−7926. (b) Mizutani, T.; Ema, T.; Yoshida, T.; Renn, T.; Ogoshi, H. *Inorg. Chem.* **1994**, *33*, 3558−3566.

(6) (a) Yashima, E.; Maeda, K.; Okamoto, Y. *Nature* **1999**, *399*, 449−451. (b) Huang, B.; Parquette, J. R. *J. Am. Chem. Soc*. **2001**, *123*, 2689−2690. (c) Prins, L. J.; De Jong, F.; Timmerman, P.; Reinhouldt, D. N. *Nature* **2000**, *408*, 181−184. (d) Ky Hirschberg, J. H. K.; Brunsveld, L.; Ramzi, A.; Vekemans, J. A. J. M.; Sijbesma, R. P.; Meijer, E. W. *Nature* **2000**, *407*, 167−170.

(7) (a) Wu, C. W.; Sanborn, T. J.; Huang, K.; Zuckermann, R. N.; Barron, A. E. *J. Am. Chem. Soc*. **2001**, *123*, 6778−6784. (b) Gin, M. S.; Moore, J. S. *Org. Lett*. **2000**, *2*, 135−138. (c) von Berlepsch, H.; Böttcher, C.; Ouart, A.; Burger, C.; Dähne, S.; Kirstein, S. *J. Phys. Chem. B* **2000**, *104*, 5255−5262. (d) Moriuchi, T.; Nishiyama, M.; Yoshida, K.; Ishikawa, T.; Hirao, T. *Org. Lett.* **2001**, *3*, 1459−1461. (e) Liu, D.; Williamson, D. A.; Kennedy, M. L.; Williams, T. D.; Morton, M. M.; Benson, D. R. *J. Am. Chem. Soc*. **1999**, *121*, 11798−11812.

(8) (a) Prince, R. B.; Brunsveld, L.; Meijer, E. W.; Moore, J. S. *Angew. Chem., Int. Ed*. **2000**, *39*, 228−230. (b) Wu, C. W.; Sanborn, T. J.; Huang, K.; Zuckermann, R. N.; Barron, A. E. *J. Am. Chem. Soc*. **2001**, *123*, 2958−2963. (c) Nakamura, K.; Okubo, H.; Yamaguchi, M. *Org. Lett*. **2001**, *3*, 1097−1099.

(9) (a) Borovkov, V. V.; Lintuluoto, J. M.; Sugeta, H.; Fujiki, M.; Arakawa, R.; Inoue, Y. *J. Am. Chem. Soc*. **2002**, *124*, 2993−3006. (b) Borovkov, V. V.; Harada, T.; Inoue, Y.; Kuroda, R. *Angew. Chem., Int. Ed.* **2002**, *41*, 1378−1381. (c) Huang, X.; Rickman, B. H.; Borhan, B.; Berova, N.; Nakanishi, K. *J. Am. Chem. Soc*. **1998**, *120*, 6185−6186. (e) Mizuno, Y.; Aida, T.; Yamaguchi, K. *J. Am. Chem. Soc*. **2000**, *122*, 5278−5285.

(10) (a) Borovkov, V. V.; Lintuluoto, J. M.; Inoue, Y. *J. Am. Chem. Soc*. **2001**, *123*, 2979−2989. (b) Borovkov, V. V.; Lintuluoto, J. M.; Inoue, Y. *J. Phys. Chem. B* **1999**, *103*, 5151−5156. (c) Borovkov, V. V.; Lintuluoto, J. M.; Fujiki, M.; Inoue, Y. *J. Am. Chem. Soc*. **2000**, *122*, 4403−4407.

(11) (a) Borovkov, V. V.; Lintuluoto, J. M.; Inoue, Y. *Org. Lett.* **2002**, *4*, 169−171. (b) Borovkov, V. V.; Lintuluoto, J. M.; Sugiura, M.; Inoue, Y.; Kuroda, R. *J. Am. Chem. Soc*. **2002**, *124*, 11282−11283.

(12) Borovkov, V. V.; Lintuluoto, J. M.; Inoue, Y. *Helv. Chim. Acta* **1999**, *82*, 919−934.

(13) Borovkov, V. V.; Yamamoto, N.; Lintuluoto, J. M.; Tanaka, T.; Inoue, Y. *Chirality* **2001**, *13*, 329−335.

(14) (a) Smith, K. M. *Porphyrins and Metalloporphyrins*; Elsevier: Amsterdam, 1975. (b) Kirksey, C. H.; Hambright, P.; Storm, C. B. *Inorg. Chem*. **1969**, *8*, 2141−2144. (c) Miller, J. R.; Dorough, G. D. *J. Am. Chem. Soc*. **1952**, *74*, 3977−3981.

(15) Kasha, M.; Rawls, H. R.; El-Bayoumi, W. A. *Pure Appl. Chem*. **1965**, *11*, 371−392.

(16) Zhou, X.; Chan, K. S. *J. Org. Chem.* **1998**, *63*, 99−104. (b) Chernook, A. V.; Shulga, A. M.; Zenkevich, E. I.; Rempel, U.; von Borczyckowski, C. *J. Phys. Chem.* **1996**, *100*, 1918−1926. (c) Sessler, J. L.; Johnson, M. R.; Lin, T.-Y.; Creager, S. E. *J. Am. Chem. Soc*. **1988**, *110*, 3659−3661.

(17) Borovkov, V. V.; Lintuluoto, J. M.; Inoue, Y. *Org. Lett.* **2000**, *2*, 1565−1568.

(18) Sugeta, H. *Bull. Chem. Soc. Jpn.* **1981**, *54*, 3706−3710.

(19) Borovkov, V. V.; Lintuluoto, J. M.; Hembury, G. A.; Sugiura, M.; Arakawa, R.; Inoue, Y. *J. Org. Chem.*, in press.

(20) It is important to note that the VT ^{1}H NMR experiment at constant host:guest molar ratio exhibits the same equilibria shift to the chiral anti form of the bis-porphyrin host as the simple increase in ligand concentration in a titration experiment.[9a,10a,c]

(21) Ponomarev, G. V.; Borovkov, V. V.; Sugiura, K.; Sakata Y.; Shul'ga, A. M. *Tetrahedron Lett.* **1993**, *34*, 2153-2156.